

# A radio-jet { galaxy interaction in 3C 441

Mark Lacy, Steve Rawlings, Katherine M. Blundell & Susan E. Ridgway

Astrophysics, Department of Physics, Keble Road, Oxford, OX1 3RH

## ABSTRACT

Multiwavelength imaging and spectroscopy of the  $z = 0.708$  radio galaxy 3C 441 and a red aligned optical/infrared component are used to show that the most striking aspect of the radio-optical alignment effect in this object is due to the interaction of the radio jet with a companion galaxy in the same group or cluster. The stellar population of the red aligned continuum component is predominantly old, but with a small post-starburst population superposed, and it is surrounded by a low surface-brightness halo, possibly a face-on spiral disc. The  $\lambda\lambda 500.7/\lambda\lambda 372.7$  emission line ratio changes dramatically from one side of the component to the other, with the low-ionisation material apparently having passed through the bow shock of the radio source and been compressed. A simple model for the interaction is used to explain the velocity shifts in the emission line gas, and to predict that the ISM of the interacting galaxy is likely to escape once the radio source bow shock has passed through. We also discuss another, much fainter, aligned component, and the sub-arcsecond scale alignment of the radio source host galaxy. Finally we comment on the implications of our explanation of 3C 441 for theories of the alignment effect.

Key words: galaxies:active { galaxies:interactions { intergalactic medium

## 1 INTRODUCTION

The consequences of radio jets impacting on density inhomogeneities have been invoked to explain many properties of high redshift radio sources, such as bending and asymmetries in arm length. Evidence for this is seen in the form of correlations between emission-line gas and the side of the radio galaxy with the shorter arm length, or higher depolarisation (McCarthy, van Breugel & Kapahi 1991; Liu & Pooley 1991). The extent to which this is related to the so-called ‘alignment effect’ whereby the axis of extended optical continuum and line emission is found to be co-aligned with the radio axis, is unclear, although many attempts to explain radio-optical alignments involve a dense external medium. Such a medium is needed, for example, to act as the source of a scattering surface for quasar light from the AGN (Bremser, Fabian & Crawford 1997), or as a medium for jet-induced star formation (e.g. Best, Longair & Rottgering 1996 & references therein).

3C 441 is a  $z = 0.708$  radio galaxy with an asymmetric radio structure, which appears to be a rare example of a radio source with a red aligned component outside the radio lobes. Such a component is clearly hard to obtain in either jet-induced star formation or scattered quasar models. This red component is seen just beyond the end of the shorter, north-west radio lobe (component ‘b’ of Eisenhardt & Chokshi (1990); see Fig. 1). This lobe appears to possess a radio jet which bends round to the west at the tip of the lobe. Just to the south of the red component, mostly within the

radio lobe, is a arc-shaped clump of emission line gas seen in the  $\lambda\lambda 372.7$  emission line image of McCarthy, van Breugel & Spinrad (1994). Spectroscopy of the  $\lambda\lambda$  emission line by McCarthy, Baum & Spinrad (1996) shows that this emission line material is redshifted by  $\sim 800 \text{ km s}^{-1}$  with respect to the radio galaxy, and weak emission extends to just beyond the red component.

In this paper, we use our own spectroscopy, infrared and radio imaging, and archive data from the Hubble Space Telescope (HST) (also presented in Best, Longair & Rottgering 1997c) to attempt to explain the properties of 3C 441 in terms of models for the interaction of radio jets with their environments. In particular, we address the problems of the origin of the red continuum light from the aligned component and the properties of the extended emission line region.

We assume an Einstein { de Sitter cosmology with a Hubble constant  $H_0 = 50 \text{ km s}^{-1} \text{ Mpc}^{-1}$ .

## 2 OBSERVATIONS

We obtained an optical spectrum with ISIS on the 4.2-m William Herschel Telescope (WHT) on 1993 August 20 with the aim of establishing the nature of component ‘b’. Both the red and blue arms of ISIS were employed, the red arm detector being the EEV5 CCD and the blue arm detector the TEK1. Observations were taken using a 3-arcsec wide slit at PA 45 deg. aligned so as to pass through both the host galaxy (‘a’ on Fig. 1) and the knot ‘b’. The aim was

Table 1. Emission line fluxes from 3C 441

Emission line	Flux in 'a'	$z_a$	Flux in 'b'	$z_c$
	$/10^{19}$		$/10^{19}$	
	$W m^{-2}$		$W m^{-2}$	
[Ne iv]242.4	1.3	0.702	< 0.5	—
[Ne v]342.6	1.7	0.7095	< 0.5	—
[O ii]372.7	4.5	0.7094	4.5	0.7132
[Ne iii]396.8	1.7	0.7084	< 0.5	—
H	0.6	0.7088	< 0.5	—
H	1.4	0.7083	< 0.9	—
[O iii]495.9	7.6	0.7084	< 0.9	—
[O iii]500.7	21.9	0.7084	2.7	0.7136
H + [N ii]	17	0.709	< 10	—

Notes:  $z_a$  and  $z_c$  are the mean redshift of the emission line in components 'a' and 'b' respectively. No aperture corrections have been applied. The optical continuum flux matched the broad-band flux measurement in a 3-arcsec diameter aperture to 20 per cent, but the infrared continuum flux was low by 0.5 mag, suggesting that an aperture correction of 1.6 should be applied to H + [N ii] flux. No attempt was made to deblend the H + [N ii] complex due to the low signal-to-noise of the detection.

between 1.02 and 1.06 and the seeing 0.9 arcsec during the observations, which consisted of a total of 3600s exposure in the blue arm and 3500s exposure in the red arm.

Observations in J- and K-bands were made with IR-CAM 3 on the United Kingdom Infrared Telescope (UKIRT) on 1996 November 6 for 20 min and 40 min respectively. Conditions were non-photometric. The seeing was 0.8 arcsec with the fast guider employed. The K-band image showed pattern noise in the form of stripes across the image, these were removed with the iraf task tld.

A J-band spectrum was obtained with CGS4 on UKIRT on 1994 June 17 covering the region of the H line. Conditions were non-photometric, with some light cirrus present. 3C 441 was observed for 3200s with the long camera and the 75  $lm m^{-1}$  grating in second order. The 2-pixel (3-arcsec) wide slit was aligned at the same PA as for the optical observations. The combined optical and infrared spectra are shown in Fig. 2.

Radio observations were made in B-array with the Very Large Array radio telescope at 8.3 GHz on 1992 January 11. The exposure time was 1950s and the bandwidth 50 MHz. The data were calibrated for phase and amplitude in the standard manner and analysed in aips. One of the two IFs was removed due to interference problems. A correction for Rician bias was made to the polarisation map using the aips task polco.

HST imaging data were obtained from the archive, and consisted of a total of 1700s exposure in the 555W and 785LP filters with the WFPC2. The radio galaxy was centered on the WF3 CCD, on which the scale is 0.1 arcsec pixel<sup>-1</sup>. The filters both contain strong redshifted emission lines: the F555W filter contains the [O ii]372.7 emission and the F785LP filter the [O iii]495.9 and 500.7 lines. Fig. 1 shows an overlay of the 8 GHz radio map contours on greyscales of the two HST images.

### 3 DISCUSSION

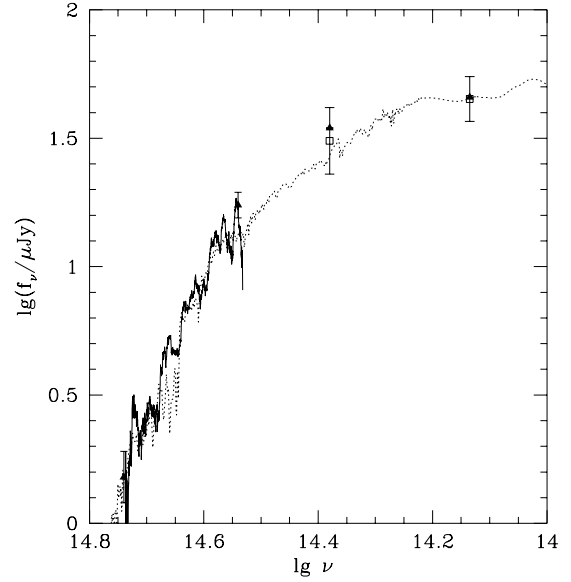


Figure 3. The SED of the compact red knot 'b'. The continuous line is from our own spectroscopy, the near infrared points from Eisenhardt & Chokshi (1990) (open squares) and our own near-infrared and optical photometry (solid triangles; note the J and K points have no associated error bars as the data were non-photometric). The dotted line is the model spectral energy distribution of a 6-Gyr old galaxy in which star formation proceeded at a constant rate in a 1-Gyr burst before ceasing (Bruzual & Charlot 1993).

#### 3.1 The continuum knot

Component 'b' in Fig. 1a and in Eisenhardt & Chokshi (1990), the red aligned knot beyond the northwest radio hotspot, is slightly resolved on the HST images. Its spectral energy distribution (SED) seems to be consistent with that of an old stellar population (Fig. 3), although the amplitude of the 4000A break seems lower than that of the model 6-Gyr old stellar population (corresponding approximately to the age of the Universe in our assumed cosmology) which is otherwise a good fit to the SED.

A stellar origin for the light is indeed confirmed by a close inspection of the spectrum of 'b' (Fig. 4) in which stellar absorption features, in particular the 'G-band' from CH absorption in cool stellar envelopes can be seen at  $z = 0.714$ , redshifted by 1000  $km s^{-1}$  with respect to the radio galaxy ( $z = 0.708$ ). Also visible are H and the calcium H and K lines, the latter possibly blended with H. The weakness of the 4000A break, despite the apparent dominance of the SED by an old stellar population may then be explained by the existence of a small post-starburst population of A-stars, and indeed the detection of H absorption in our spectrum is consistent with this. Such populations have been detected in other AGN host galaxies and companions (Tadhunter, Dickson & Shaw 1996; Canalizo & Stockton 1997), and may trace mergers or interactions in small clusters or groups (Zabludov et al. 1996).

Whether there is a link between a starburst 10<sup>8</sup> yr ago in a close companion or the host itself and the triggering of the AGN is unclear (certainly if so there must be a delay between the starburst and the development of a radio source if typical radio source lifetimes are 10<sup>7</sup> yr (Alexander &

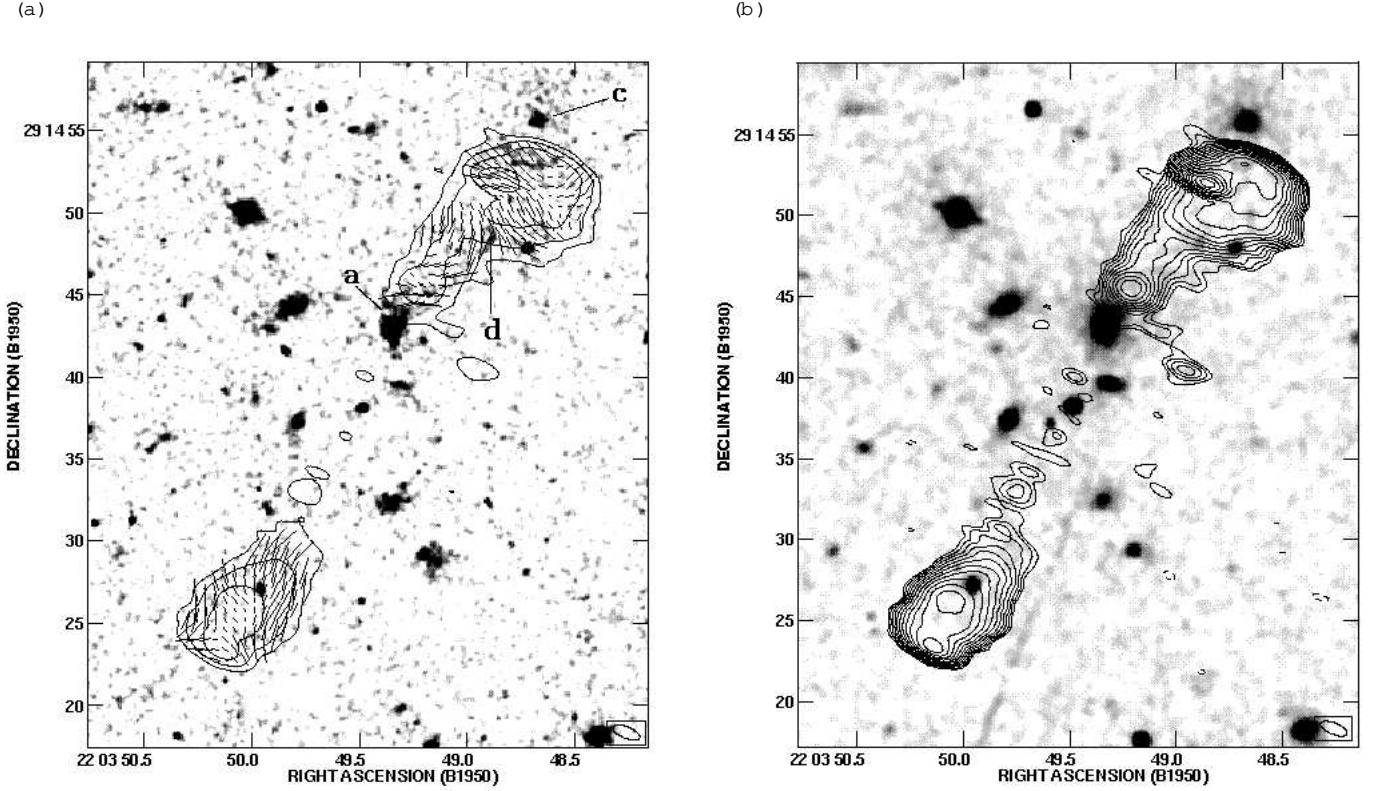


Figure 1. Overlay of the WFC2 images of 3C 441 on our VLA 8 GHz B-array radio map. (a) The F555W image smoothed with a  $\sigma = 0.1$  arcsec Gaussian, with radio contours and magnetic field polarisation vectors superposed. The optical components referred to in the text are labelled. Contours are spaced at intervals separated by factors of four from  $0.4 \text{ mJy beam}^{-1}$ , and the polarisation vectors are scaled so that a length of 1 arcsec represents 25 per cent polarisation. (b) The F785LP image smoothed with a Gaussian with  $\sigma = 0.2$  arcsec, with radio contours again superposed. Contours are spaced at intervals separated by factors of  $2^{1/2}$  starting at  $0.3 \text{ mJy beam}^{-1}$ . The radio beam FWHM is indicated in the bottom right corner of both plots.

Leahy 1987). In the case of 3C 441, component  $\nu'$  is  $\sim 125$  kpc from the host galaxy, so it is conceivable that if its relative velocity with respect to the host in the plane of the sky is of the same order as its relative velocity along the line of sight, it could have been close enough to interact  $10^8$  yr ago. There is, however, no sign of a corresponding starburst in the host galaxy, and E+A galaxies are relatively common in high- $z$  clusters (Dressler & Gunn 1990; Caldwell & Rose 1997). Furthermore, the high velocity encounter implied by this may not have produced sufficient disruption to initiate the starburst.

### 3.2 The emission line gas in $\nu'$

Contour plots of the 2-D spectra around the  $\text{H}\beta$  4861 and  $\text{H}\gamma$  4340 emission lines are shown in Fig. 5. There is a striking change in the ionisation and luminosity across the position of the continuum knot: the side nearest to the radio galaxy has a high luminosity, and a low ionisation as measured by the ratio of  $\text{H}\gamma/\text{H}\beta$  emission lines (0.35–0.1). In contrast, beyond the knot the  $\text{H}\gamma/\text{H}\beta$  ratio is much higher ( $> 10^{-3}$ ) and the total luminosity lower by a factor of  $\sim 6$ . There is a velocity gradient of  $\sim 300 \text{ km s}^{-1}$  in the line emission across the continuum knot, in the sense that the side nearest the radio galaxy is blueshifted, and that on the far side is, within

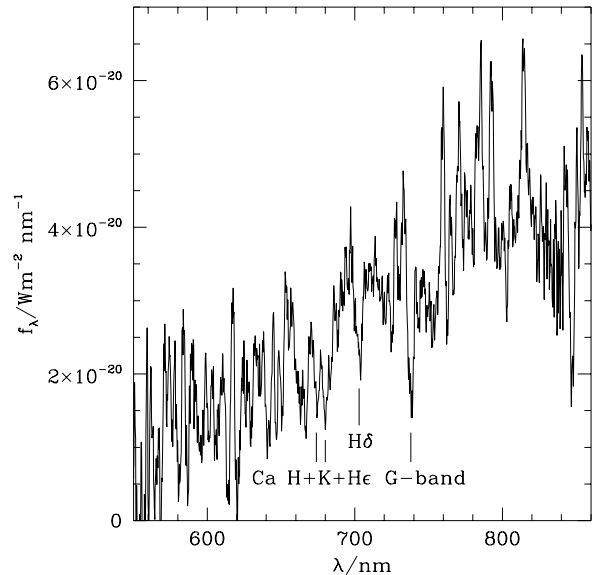


Figure 4. The red-arm spectrum of knot  $\nu'$  of 3C 441, showing the stellar absorption features mentioned in the text. The raw spectrum has been smoothed by a 9-pixel (2.4 nm) box-car filter and corrected for atmospheric absorption.

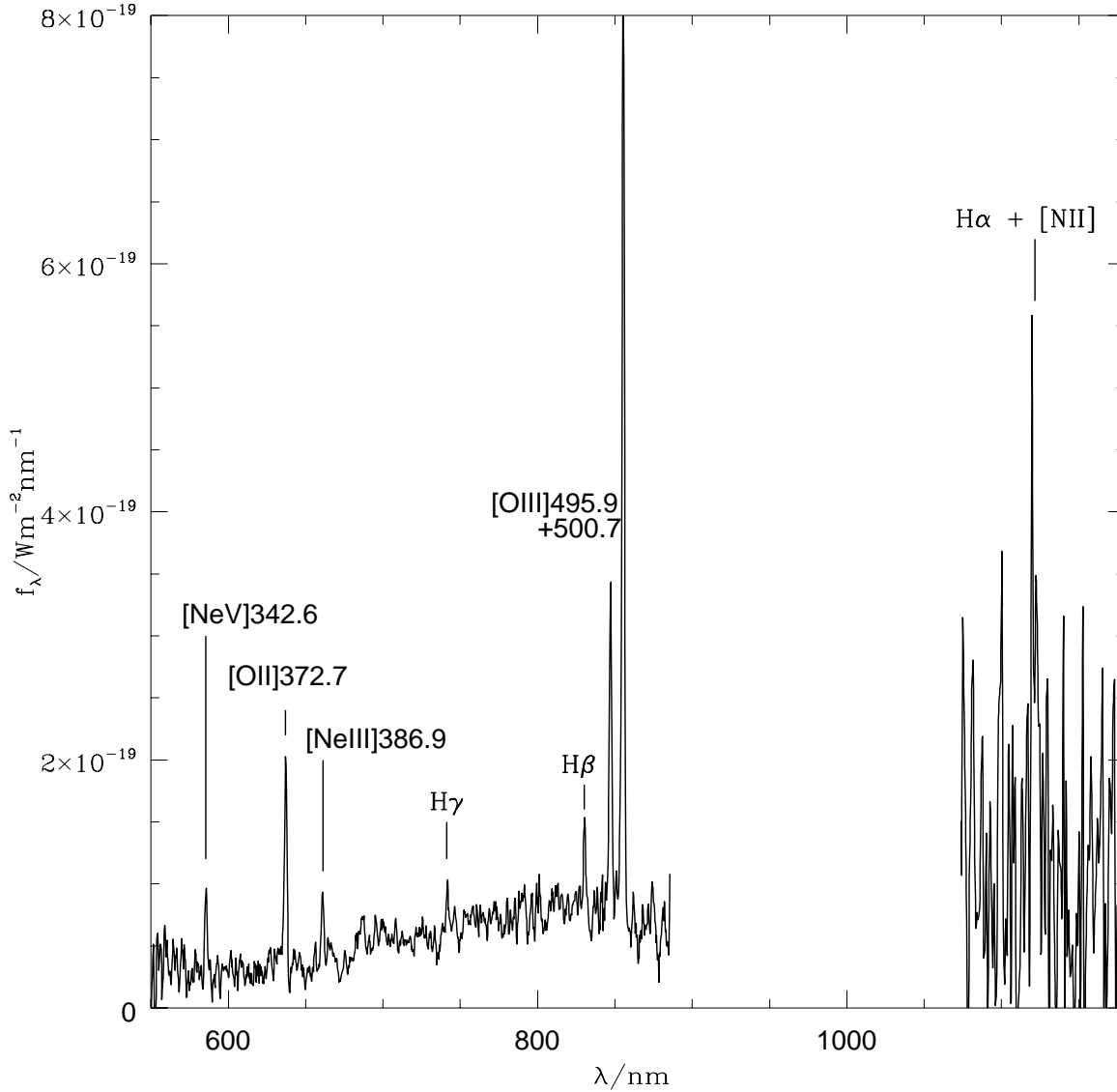


Figure 2. The spectrum of the radio galaxy  $\lambda'$ . The ISIS red-arm optical spectrum has been smoothed with a 5-pixel (1.4 nm) box-car filter and the CGS4 near-infrared spectrum by a 9-pixel (7.2 nm) one.

errors of  $100 \text{ km s}^{-1}$ , at rest with respect to the starlight in  $\lambda'$ . There is also a faint tail of yet more highly blueshifted emission (up to  $600 \text{ km s}^{-1}$ ) on the side nearest the radio galaxy, pointing towards the radio galaxy.

Note that there is no sign of emission lines in Fig. 4, which used a narrow extraction about the continuum peak. In contrast, in Fig. 5 the extended emission-line flux from  $\lambda'$  is clearly visible and is quite strong when integrated over the entire emission region (Table 1).

### 3.3 The radio structure

The asymmetric radio structure of 3C 441 is interesting in the context of the models to explain the aligned emission. The asymmetry in jet brightness either side of the nucleus is very pronounced, and can be interpreted either as an asymmetry produced by Doppler boosting, or in terms of 3C 441 having a radio structure transitional between FR I and FR II, with one side FR II-like and the other more FR I-like. The lack of a radio central component, common only seen in ra-

dio galaxies with Doppler boosted one-sided jets (e.g. 3C 22, Rawlings et al. 1994), argues strongly in favour of the latter explanation, and indeed the aring of the jet just to the NW of the host galaxy is reminiscent of the "Mach disk" structure seen in the M 87 jet (Owen, Hardee & Cornwell 1989).

### 3.4 The radio galaxy

The spectrum of  $\lambda'$ , the host galaxy of the radio source is shown in Fig. 2. It is a typical moderately-high ionisation narrow-line radio galaxy spectrum, with strong emission lines superposed on a stellar spectrum dominated by an old stellar population with a strong 4000Å break.

Close inspection of the images shows, however, that even in this case, where the integrated light is dominated by old stellar populations there is evidence for morphological peculiarity. In particular there is a distinct blue aligned component to the south east of the host galaxy peak (Fig. 6). Whether this represents a spiral arm, a merger remnant

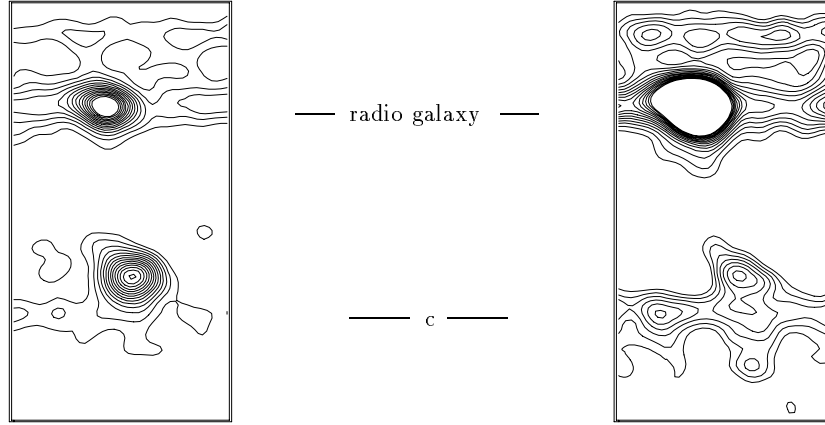


Figure 5. 2-D spectrum of 3C 441 with the slit aligned along the axis joining the radio galaxy and  $b'$ . Left: the [O II] emission line with wavelength on the horizontal axis and distance along the slit vertically. The radio galaxy is to the top and component  $b'$  below it. Right: the [O III]5007 emission line. The figures are  $11.2 \text{ nm} \times 30 \text{ arcsec}$  in size ( $11.2 \text{ nm} = 5280 \text{ km s}^{-1}$  close to [O II] and  $3930 \text{ km s}^{-1}$  close to [O III]). The contour levels are spaced at intervals of  $2 \times 10^{-21} \text{ W m}^2 \text{ nm}^{-1}$  per pixel, starting from  $2 \times 10^{-21} \text{ W m}^2 \text{ nm}^{-1}$ , each pixel was  $0.28 \text{ nm} \times 0.33 \text{ arcsec}$  in size.

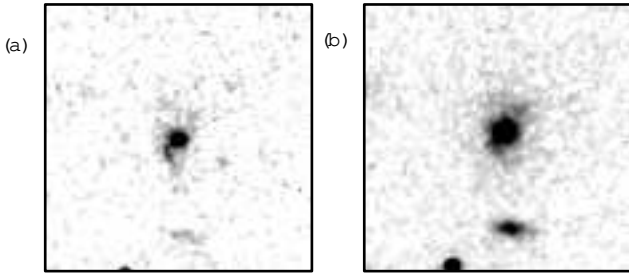


Figure 6. Close-up of the host galaxy ( $a'$ ) greyscaled so as to show the aligned components near the nucleus: (a) F555W image; (b) F785LP image. Both images are 10 arcsec square and have been smoothed with a  $\sigma = 0.05 \text{ arcsec}$  gaussian.

or some form of radio source-induced aligned component is unclear. As its separation from the radio galaxy is only about 0.5-arcsec, it is hard to tell from the spectra whether it is line or continuum dominated, but the more diffuse material extending 2-arcsec to the south of the radio galaxy is definitely continuum dominated. Although much weaker relative to the smooth underlying host galaxy in the F785LP image, the aligned component is nevertheless visible, along with some more diffuse aligned emission on the other side of the peak, to the northwest.

In Fig. 7, the position angle of the host galaxy (derived from the second moments of the flux distribution) is plotted for various isophotes and apertures. This shows two interesting aspects of the alignment. First, the alignment persists into the K-band, suggesting the aligned light is fairly red. Second, in the HST images, there is evidence for isophotal twisting as the aperture size is increased to include the inner aligned components highlighted in Fig. 6 (PA  $\sim 150^\circ$ ), and later the low surface brightness emission round the host at PA  $\sim 0^\circ$ , seen best in Fig. 1. The low-surface brightness material to the northwest may be mostly line emission though, as the emission-line image of McCarthy et al. (1995) shows that the [O II] emission is also roughly aligned along PA  $0^\circ$ .

### 3.5 The relationship of the radio and optical components

The relative astrometry was performed using the results of the APM scans of the Palomar Sky Survey plates. The positions of four stars were used to align the corners of the radio map with the optical images. The uncertainty in the overlay from the scatter in the fit was  $0.3 \text{ arcsec}$ . This astrometry places the host galaxy ( $a'$  in Fig. 1a) just to the SE of the first appearance of the northern radio jet. Component  $b'$  is apparently aligned along the jet direction, although positioned to the side of it. The point of deflection of the jet is approximately coincident with the peak of the [O II]372.7 emission, about 3-arcsec SE of the peak of the continuum knot  $b'$ . In the F555W image (Fig. 1a), there is an arc of emission just to the north of the north-west radio hotspot and apparently centered on  $b'$ . Fig. 1b shows the F785LP image; here there is a halo of diffuse emission around  $b'$ .

By subtracting a spectrum centered on the continuum knot in an aperture 1.7-arcsec wide from the total spectrum of the aligned component  $b'$  (in a 6.8-arcsec wide aperture), we have been able to estimate the line contribution to the continuum magnitudes measured for the nebular region surrounding  $b'$ . In both filters this is 10 per cent overall, but in the regions of brightest line emission in the interaction region to the south of  $b'$  our spectrum suggests that the line contribution of [O II] to the F555W flux rises to dominate the overall flux in the filter, consistent with the arc of emission seen in the F555W region just above the radio hotspot consisting entirely of line emission. The continuum emission present in this extraction is bluer than the emission from the knot.

The linear object  $b'$  (Fig. 8) is reminiscent of the aligned component in 3C 34 (Best, Longair & Rottgering 1997a). Like the object in 3C 34, it has no emission lines visible either in our spectra or in the narrow-band image of McCarthy et al. (1994), but is well aligned with the radio structure and lies within the radio lobe. Its optical { near infrared colours are bluer than  $b'$  ( $K = 20.3; J > 22.7; m_{785} = 23.3; m_{555} = 25.1$  in 3-arcsec diameter aper-

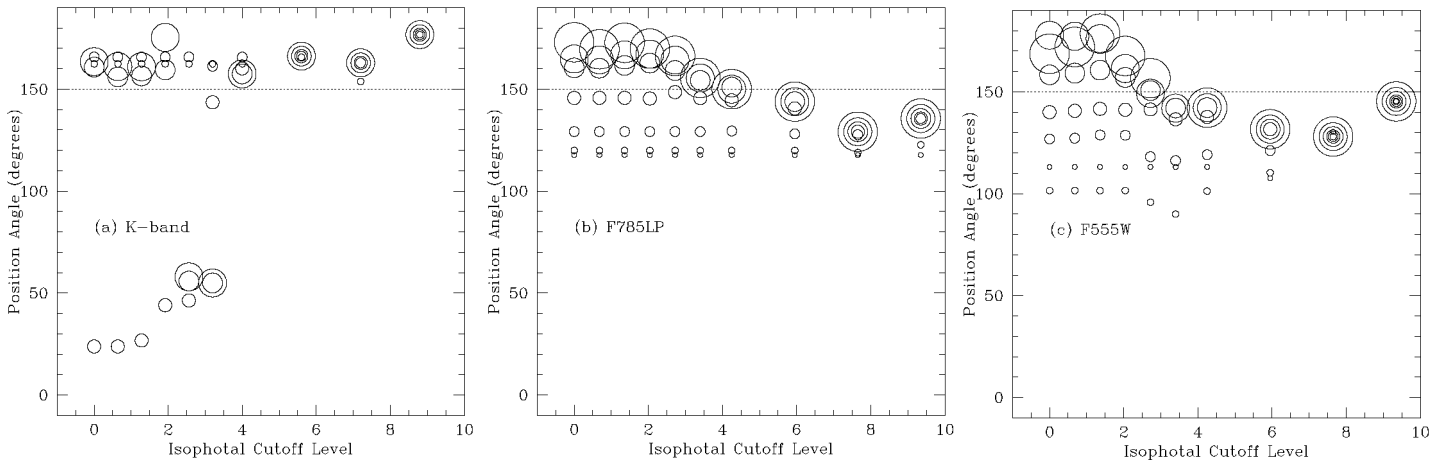


Figure 7. Position angle as a function of aperture size and isophotal cutoff for the host galaxy of 3C 441. The isophotal cutoff level is in units of the sky noise, and the aperture radii (indicated by circles of increasing size) are 0.6, 0.9, 1.1, 1.7 and 2.4 arcsec in (a), and 0.3, 0.4, 0.6, 0.8, 1.2, 1.7, and 2.4 arcsec in (b) and (c). The radio source PA (defined as the PA of the line joining the hotspots) is indicated by a dotted line.

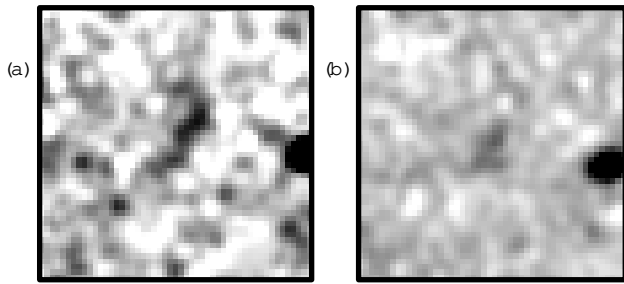


Figure 8. Close-up of component 'b': (a) F555W image; (b) F785LP image. Both images are 5 arcsec square and have been smoothed with a  $\sigma = 0.1$  arcsec Gaussian.

tures, where  $m_{785}$  and  $m_{555}$  are AB magnitudes in the two HST images, but show a break between the 785LP and 555W filters, consistent with a 4000 Å break at the redshift of the radio source.

### 3.6 Other companion objects

There are several objects around the radio galaxy which appear to be members of a group or cluster around it. 3C 441 is in a sample of radio galaxies whose clustering properties we are currently evaluating, and a formal estimate of the clustering amplitude,  $B_{gg}$ , for this radio source will be presented in Wolf et al. (in preparation). For the purposes of this paper, we simply compared the counts of galaxies with magnitudes  $m_1$  to  $m_1 + 3$  (where  $m_1$  is the magnitude of the radio source host galaxy) in the object frame of the F785LP image (the WF3 CCD) with the average of those in the two side frames (WF2 and WF4). This revealed an excess of 11.5  $\pm$  7.1 galaxies, indicating the possible presence of a cluster, but not at a high confidence level. Clearly though this is likely to be an underestimate of the cluster richness as many cluster members may be outside the restricted field

of the CCD, and present on the other frames, increasing the estimate of the background count.

## 4 INTERPRETATION OF THE ALIGNED STRUCTURES

### 4.1 Component 'b'

We argue here that the evidence presented above allows us to deduce that 3C 441 includes an example of a radio-jet { galaxy interaction. Best et al. (1997c) have also proposed a jet (galaxy interaction at 'b', but were unable to confirm it using the HST imaging data alone.]

First, the evidence that the northern radio jet is being deflected by an increase in density just south of knot 'b' is given by the fact that the radio jet appears to bend round to the west  $\sim 3$  arcsec SE of 'b', consistent with simulations of radio jets interacting with gas clouds (Higgins, O'Brien & Dunlop 1997). The polarisation B-field vectors (Fig. 1a) are also consistent with an interaction scenario, tending to be perpendicular to the emission-line arc. The relatively high polarisation of the interaction region (up to 30 per cent) suggests that we are seeing the interaction through the radio lobe (contrast PKS 2250-41; Clark et al. 1997, in which the polarisation of the interacting lobe at 8 GHz is only 2.6 per cent, so in that case the emission line gas is almost certainly covering the radio lobe). Provided the rotation measure is  $200 \text{ rad m}^{-2}$  in the rest-frame of the source, the angle of polarisation will be rotated by  $\sim 5^\circ$ .

Second, the evidence that the radio jet is shocking the emission-line gas to the south of knot 'b' is strong. The fact that emission-line gas is present beyond the interaction region shows that photoionisation is probably responsible for most, if not all, of the line emission. The main photoionisation mechanism could either be photoionisation by the nucleus, or photoionisation by hot, post-shocked gas. Hot stars in H II regions of the galaxy could also contribute to the

photoionising flux. Irrespective of the ionisation mechanism, compression of the shocked gas would lead to a decrease in the ionisation parameter (Clark et al. 1997), and hence the difference in ionisation between the two sides of knot B'. The velocity structure of the emission lines is also consistent with shocking, with the emission being blueshifted on the radio galaxy side of the continuum knot, suggesting that the radio jet is approaching the observer. The mean velocity of the knot, a redshift of  $+1000 \text{ km s}^{-1}$  is assumed to come from the random motion of the galaxy in a cluster around 3C 441.

Third, the halo-like appearance of the diffuse emission around a central continuum knot and the distribution of [O III]500.7 emission in the spectrum is hard to explain unless the stars and gas are associated with a galaxy. This galaxy has an red old or E+A-type central concentration of stars with a surrounding lower surface-brightness disc or halo, in which there is a significant quantity of gas. The spectrum of the diffuse emission shows that the SED of the extended continuum is consistent with that of a late-type spiral, with rest-frame  $U - B = 0.2$  (Coleman, Wu & Weedman 1980). The most straightforward interpretation of this is therefore that we are seeing the interaction of the radio jet with a face-on spiral galaxy in the same cluster, with the bulge component providing the central high surface brightness knot of red light (with little gas to provide line emission from this region) and the gas and stars in the surrounding disk providing the diffuse halo of emission. The [O II] emission, however, appears to trace the bow-shock, presumably due to compression behind the shock increasing the density and lowering the ionisation parameter. The size of the disk (44 kpc in our assumed cosmology) is typical of the size of a spiral disk seen in H I (e.g. Broeils & van Woerden 1994). The problem of survival of the gas halo or disk in the cluster environment that may surround 3C 441 suggests that the galaxy may only recently have fallen into the cluster.

#### 4.2 A simple model for the interaction

We consider a simple model in which the radio jet interacts with a two-phase interstellar medium of the spiral galaxy. Similar models have been developed to investigate the interactions of supernova shocks with the interstellar medium, and the case of the interaction of radio jets with a two-phase medium has been discussed by Rees (1989). These models show that the shock wave propagates through the hot phase, initially by-passing the cold clouds (in which the shock speed is much lower). The velocity given to the cold clouds can be estimated by considering the effect of the pressure differential as the shock passes. For a cloud of radius  $r$  and a jump in pressure  $P$  across a shock of speed  $v_{sh}$ , the velocity given to the cloud,

$$v_{cl} = r^2 P \frac{1}{v_{sh}} \frac{1}{\rho_{cl} r^3} = \frac{P}{\rho_{cl} M c_h}$$

where  $\rho_{cl}$  is the density of the cold clouds,  $M$  the Mach number of the shock (in the pre-shock medium) and  $c_h$  the speed of sound in the hot-phase gas (i.e. independent of the size of the cloud). From the limiting forms of the Rankine-Hugoniot relations in the case of a strong shock,

$$P = P_1 M^2$$

where  $P_1$  is the preshock gas pressure. Hence

$$v_{cl} = \frac{P_1 M}{\rho_{cl} c_h} \frac{c_{cl}^2}{c_h^2} v_{sh} = 100 \frac{T_{cl}=10^4 \text{ K}}{T_h=10^6 \text{ K}} (v_{sh}=10^4 \text{ km s}^{-1}) \text{ km s}^{-1}$$

where  $T_{cl}$  and  $T_h$  are the temperatures of the cold and hot phases respectively. If we take  $v_{sh} = v_{rs} = 0.03c$ , typical for a radio source advance speed (Alexander & Leahy 1987), this process can easily account for the modest velocity shifts seen in the gas to the south of the knot relative to the unshocked gas in the north.

The ionisation parameter (here defined as the dimensionless ratio of the number density of photoionising photons to the total number density of hydrogen atoms,  $U = n_{ph}/n_H$ ) will change across the shock as  $n_H$  is increased ( $n_{ph}$  is likely to be similar either side of the knot whether the ionisation is due to shocks or to the nucleus). Typically [O III]500.7/[O II]372.7 is expected to be a linear function of  $U$  over the range we are considering (e.g. Penston et al. 1990). To obtain the observed change in the [O III]500.7/[O II]372.7 ratio therefore requires an enhancement of  $n_H$  in the post-shock region by a factor of  $\sim 30$ . This demonstrates the importance of the two-phase assumption: if only one phase were present the Rankine-Hugoniot relations predict a density enhancement of at most a factor of 4. The cloud gas should also be heated by the compression following the shock, but deeper spectroscopy is required to measure the [O III]436.3 temperature diagnostic line either side of the shock.

Numerical simulations (e.g. Stone & Norman 1992, who examine the physically-similar situation of supernova shocks) show that in fact the hot phase, which is moving at a high speed with respect to the cold clouds interpenetrates the cold medium and eventually (within a few sound-crossing times of the cloud) causes turbulent mixing of the hot and cold phases. This is probably required to produce the high velocity tail of blueshifted emission line gas. Gas with high velocity shifts and widths ( $\sim 1000 \text{ km s}^{-1}$ ) is seen in a number of high- $z$  radio galaxies, e.g. 3C 368, and probably arises from this mechanism (Stockton, Ridgway & Kellogg 1996; Tadhunter 1997).

#### 4.3 Component B'

The apparent close correlation of the position angle of B' with the direction of the radio structure may of course be coincidental, and B' may well be a companion, foreground or background galaxy which just happens to align with the radio axis. In section 3.5 we showed that the colours of B' were at least consistent with it being in the same group or cluster as the radio galaxy and B', but there is no other evidence to associated B' with these two galaxies. Nevertheless, we can speculate on what B' might be if its alignment is not a coincidence.

One possible explanation is that B' may be a tidal remnant of an encounter between the radio galaxy and B' (see Section 3.1). If, however, as previously argued any interaction of the radio galaxy and B' is unlikely to have been very disruptive, this leaves the possibility that the alignment of B' is caused by a process involving the radio source, most

plausibly either starlight produced by jet-induced star formation, or optical synchrotron emission.

If  $\ell'$  is synchrotron emission, it is not emission from the jet centre, which clearly passes to one side. Emission from a boundary layer of the jet cannot be ruled out, however, and indeed an interaction of the boundary layer of the jet with a galaxy or gas clump might be expected to be a region of high magnetic field and current particle acceleration, in a manner analogous to that seen in supernova remnants (e.g. Anderson et al. 1994). We nevertheless cannot rule out a jet-induced star formation origin for this component, on the lines of that proposed by Best et al. (1997a) for the similar component in 3C 34. Probably the best argument against this (apart from the lack of emission lines) is that the object is parallel to the current jet direction, not the line joining it to the host galaxy as one might naively expect if the galaxy was formed as a result of an interaction with the head of the expanding radio source.

#### 4.4 The host galaxy

Although relatively subtle, as Fig. 7 demonstrates, the light from the host of 3C 441 is aligned along the direction of the radio jet in both HST passbands (which straddle the 4000Å break) and in the near-infrared. The fraction of aligned light (defined here as the fractional excess of emission within  $\pm 22.5^\circ$  of the radio axis) is largest in the F555W image, at about 20 per cent, falling to ten per cent in the F785LP image and only four per cent in the K-band. Thus although 3C 441 is one of the least "active" [by the definition of Best et al. (1997b)] galaxies in 3C, and has no detectable polarisation in the infrared to a limit of  $\sim 5$  per cent (Leyshon & Eales 1997), we cannot eliminate the possibility that the aligned light is scattered. Nebular continuum is unlikely to contribute though, because the observed limit on the H $\alpha$  emission suggests that nebular continuum accounts for  $< 1$  per cent of the total K-band flux, and, although in the optical emission lines may contribute to the aligned components, there is no strong emission line in K-band.

The aligned structures themselves are not closely associated with visible radio emission, rendering both synchrotron and inverse-Compton mechanisms (Daly 1992) unlikely. Jet-induced star formation, however, cannot be ruled out here, although the colour difference between the aligned emission north and south of the galaxy argues somewhat against this, as in the jet-induced star formation model stellar populations at equal distances from the nucleus should have similar colours. However, differential dust extinction either side of the nucleus could be responsible for the colour difference.

The aligned structure seen particularly in the F555W image (Fig. 6a) is a particularly intriguing feature of this object, reminiscent of the more spectacular features in 3C 280 (Ridgway & Stockton 1997). As it seems fairly blue, it may represent an AGN-produced component, or pre-existing material brightened by the interaction with the radio jet, for example nebular continuum emission from shocked gas, and it may therefore contribute little to the near-infrared aligned light.

The presence of a good near-infrared alignment may imply a link between the position angle of the underlying old stellar population and the radio jet axis, perhaps produced by a selection effect (Eales 1992). Evidence in favour of this

is the surprisingly good correlation often seen in 3C radio galaxies between the infrared PA and the radio axis. Dunlop & Peacock (1993) even claim that it is better than that seen in the optical. Although subsequent HST studies have shown some of Dunlop & Peacock's infrared alignments to be fortuitous (e.g. 3C 175.1; Ridgway & Stockton 1997), it is also clear that in some cases (e.g. 3C 280; Ridgway & Stockton 1997), the infrared emission may be well aligned even after subtraction of some extended aligned components seen in the optical.

Alignments between cD galaxies and the projected distribution of galaxies within clusters have been noted by Rhee, van Haarlem & Katgert (1992). Given the common occurrence of clusters around radio sources at  $z \sim 0.5$ , it seems not unlikely that the central galaxy is aligned with the cluster potential, and the selection effect pointed out by Eales (1992) will then tend to favour aligned radio sources [but see West (1994) for an alternative explanation of the alignment of the radio source with the cluster/cD axis].

## 5 IMPLICATIONS OF RADIO-SOURCE GALAXY INTERACTIONS

3C 441 is a striking example of the "alignment effect" whereby the radio and optical axes of  $z > 0.7$  powerful radio galaxies are frequently found to be co-aligned. In this case, if we are correct, the most spectacular aspect of the alignment, that of knot  $\ell'$  with the radio axis, has a relatively simple explanation – namely the interaction of the radio jet with another galaxy in the same group or cluster. A jet-galaxy interaction has also been invoked to explain the properties of the aligned emission in the  $z = 0.3$  radio galaxy PKS 2250-47 (Clark et al. 1997). How relevant these are to the more problematic cases seen at higher redshifts (and usually higher radio powers too) is unclear. For example, the host galaxy and knot  $\ell'$  of 3C 441 are  $< 5$  per cent polarised (Tadhunter et al. 1992; Leyshon & Eales 1997), but in many examples of high- $z$  radio galaxies the aligned light has a polarisation of  $\sim 10$  per cent. Also, there are very few examples where the aligned component is outside the radio lobes.

Jet-induced star formation, the process whereby radio jets impacting on gas clouds promote star formation, appears not to be happening in the aligned component  $\ell'$  of 3C 441. Although the appropriate conditions appear to be in place (namely a powerful radio jet impacting on dense clouds of gas), there is apparently no significant extra blue continuum associated with the interaction region that might come from a population of very young stars (the youngest stellar population detectable in  $\ell'$  is the spiral disc population, which is equally bright on both sides of the central knot). However, it may simply be that the interaction has occurred too recently for the stars to begin to form.

The effects of the interaction on galaxy  $\ell'$  may be dramatic. The post-shock temperature of the hot ( $10^6$  K) component of the ISM of  $\ell'$  will be raised as it passes through the shock by a factor  $M^2 = 4$ . Assuming  $v_{\text{sh}} \sim 10^4 \text{ km s}^{-1}$ , this is a factor of  $\sim 10^3$ . Mixing with the cold medium and radiative losses will cool it somewhat, but it is likely that the resulting gas will still have thermal velocities exceeding the galaxy escape velocity (corresponding to  $T \sim 10^4$  K),



and will ultimately evaporate into the intracluster medium (ICM). Thus radio source interactions may provide a method of stripping gas from cluster galaxies, and thereby adding metal-enriched gas to the ICM.

The importance of jet { companion galaxy interactions in producing radio { optical alignments is still to be fully quantified. It is likely that interactions of this sort produce large amounts of line emission and some nebular continuum, and, if they occur close to the nucleus, the continuum emission will be further brightened by scattering of the hidden quasar light. Any old stellar population in the companion galaxy contributes light in the near infrared, and, if the selection effect pointed out by Eales (1992) is effective, we would expect to see more companion galaxies along the radio axes than elsewhere. Furthermore, if radio galaxies form by the accumulation of smaller sub-units as in the "bottom-up" structure formation hierarchy, close companions will be a common feature of high- $z$  radio galaxy hosts.

#### ACKNOWLEDGEMENTS

We thank Chris Simpson for assistance with the UKIRT observations. We are also grateful to the support staff at the WHT and UKIRT for their help with the observations. We also thank the referee for a number of useful comments. This paper was partly based on observations made with the NASA/ESA Hubble Space Telescope, obtained from the data archive at the Space Telescope Science Institute. STScI is operated by the Association of Universities for Research in Astronomy, Inc. under the NASA contract NAS 5-26555. The National Radio Astronomy Observatory is a facility of the National Science Foundation operated under cooperative agreement by Associated Universities Inc. The WHT is operated on the island of La Palma by the Royal Greenwich Observatory in the Spanish Observatorio del Roque de los Muchachos of the Instituto de Astrofísica de Canarias, and the UKIRT by the Royal Observatory Edinburgh on behalf of the UK PPARC. We are grateful to Mike Irwin and Richard McMahon for making the APM scans of the Palomar Sky Survey generally available.

#### REFERENCES

- Alexander P., Leahy J.P., 1987, *MNRAS*, 225, 27  
 Anderson M.C., Jones T.W., Rudnick L., Tregillis I.L., Kang H., 1994, *ApJ*, 421, L31  
 Barthel P.D., 1989, *ApJ*, 336, 606  
 Best P.N., Longair M.S., Rottgering H.J.A., 1996, *MNRAS*, 280, L9  
 Best P.N., Longair M.S., Rottgering H.J.A., 1997a, *MNRAS*, 286, 785  
 Best P.N., Longair M.S., Rottgering H.J.A., 1997b, *astro-ph/9703055*  
 Best P.N., Longair M.S., Rottgering H.J.A., 1997c, *astro-ph/9707337*  
 Bremer M.N., Fabian A.C., Crawford C.S., 1997, *MNRAS*, 284, 213  
 Broeils A.H., van Woerden H., 1994, *A&AS*, 107, 129  
 Bruzual A.G., Charlot S., 1993, *ApJ*, 405, 538  
 Caldwell J.A., Rose N., 1997, *AJ*, 113, 492  
 Canalizo G., Stockton A.N., 1997, *ApJ*, 480, L5

- Clark N.E., Tadhunter C.N., Morganti R., Killean N.E.B., Fosbury R.A.E., Hook R.N., Siebert J., Shaw M.A., 1997, *MNRAS*, 286, 558  
 Coleman G.D., Wu C.-C., Weedman D.W., 1980, *ApJS*, 43, 393  
 Daly R.A., 1992, *ApJ*, 386, L9  
 Dressler A., Gunn J.E., 1990, in: Kron R.G., ed, *Evolution of the Universe of Galaxies*. Astronomical Society of the Pacific, p. 200  
 Dunlop J.S., Peacock J.A., 1993, *MNRAS*, 263, 936  
 Eales S.A., 1992, *ApJ*, 397, 49  
 Eales S., Rawlings S., 1993, *ApJ*, 411, 67  
 Eisenhardt P., Chokshi, A., 1990, *ApJ*, 351, L9  
 Higgins S., O'Brien T., Dunlop J., 1996, in: Ekers R., Fanti C., Padrielli L., eds, *Proc. IAU 175, Extragalactic Radio Sources*. Kluwer Dordrecht, p. 467  
 Leyshon G., Eales S., 1997, *astro-ph/9708085*  
 Liu R., Pooley G., 1991, *MNRAS*, 253, 669  
 McCarthy P.J., Baum S.A., Spinrad H., 1996, *ApJS*, 106, 281  
 McCarthy P.J., van Breugel W., Kapahi V.K., 1991, *ApJ*, 371, 478  
 McCarthy P.J., van Breugel W., Spinrad H., 1995, *ApJS*, 99, 27  
 Owen F.N., Hardee P.E., Comwell T.J., 1989, *ApJ*, 340, 698  
 Penston M.V., et al., 1990, *A&A*, 236, 53  
 Rawlings S., Lacy M., Sivia D.S., Eales S., 1994, *MNRAS*, 274, 976  
 Rees M.J., 1989, *MNRAS*, 239, 1P  
 Rhee G., van Haarlem M., Katgert P., 1992, *AJ*, 103, 1721  
 Ridgway S.E., Stockton A.N., 1997, *AJ*, 114, 511  
 Scheuer P.A.G., 1995, *MNRAS*, 277, 331  
 Stockton A.N., Ridgway S.E., Kellogg M., 1996, *AJ*, 112, 902  
 Stone J.M., Norman M.L., 1992, *ApJ*, 390, L17  
 Sutherland R.S., Bicknell G.V., Dopita M.A., 1993, *ApJ*, 414, 510  
 Tadhunter C.N., 1997, in: Clark N., ed, *Jet-cloud interactions in active galaxies*. <http://www.shef.ac.uk/~phys/research/astro/conf/tadhunter/tadhunter.html>  
 Tadhunter C.N., Dickson R.C., Shaw M.A., 1996, *MNRAS*, 281, 591  
 Tadhunter C.N., Scarrott S.M., Daper P., Rolph C., 1992, *MNRAS*, 256, 53  
 West M.J., 1994, *MNRAS*, 268, 79  
 Zabludov A.I., Zaritsky, D., Lin, H., Tucker, D., Hashimoto, Y., Shethan, S.A., Oemler, A., Kirshner, R.P., 1996, *ApJ*, 466, 104